Radially Accelerated Trajectories for Variable Mass Spacecraft

Alessandro A. Quarta *, Giovanni Mengali

Department of Civil and Industrial Engineering, University of Pisa, I-56122 Pisa, Italy

Abstract

This paper proposes a new approach for mission design of a spacecraft with a time-variable mass and subjected to a continuous propulsive thrust in the radial direction. Two different mission scenarios are discussed according to whether the thrust remains constant along the whole mission or its modulus varies inversely proportional to the distance between the spacecraft and the primary body. In the first case a graphical solution is discussed for evaluating the spacecraft performance during an escape mission scenario. In the second case a closed-form solution, which makes use of the trigonometric integral functions, is found for describing the spacecraft trajectory in a polar reference frame. Some examples are discussed where the methodology is applied to a spacecraft with an electric thruster or a mini-magnetospheric propulsion system.

Key words: Radial thrust, Escape trajectory, Electric thruster, M2P2 propulsion system.

* Corresponding author.
Email addresses: a.quarta@ing.unipi.it (Alessandro A. Quarta), g.mengali@ing.unipi.it (Giovanni Mengali).

Nomenclature

a	=	propulsive acceleration
$\mathcal{E}$	=	specific mechanical energy
g	=	standard gravity
h	=	specific angular momentum
I_{sp}	=	specific impulse
m	=	spacecraft mass
O	=	primary body center-of-mass
r	=	radial distance
$\boldsymbol{T}$	=	propulsive thrust (with $T \triangleq \|\boldsymbol{T}\|$)
$\mathcal{T}(O; r, \theta)$	=	polar reference frame
u	=	radial component of spacecraft velocity
v	=	circumferential component of spacecraft velocity
v_e	=	effective exhaust velocity
γ	=	Euler's constant
θ	=	polar angle
μ	=	gravitational parameter
ρ	=	auxiliary variable

Subscripts

0	=	initial, parking orbit
esc	=	escape
$\oplus$	=	Earth
$\odot$	=	Sun

Superscripts

$\cdot$ = time derivative

$\sim$ = dimensionless

$'$ = derivative w.r.t. $\widetilde{m}$

1 Introduction

Analytical solutions of trajectories for low-thrust-propulsion spacecraft are known in a few cases only. One of these is offered by the classical problem of a spacecraft, with constant mass, subjected to a radial thrust. Starting from the pioneering work of Tsien [1], some interesting results of this problem have been reported for a constant modulus of the propulsive acceleration [2,3,4]. Other results are available for a radial propulsive acceleration whose modulus varies as the inverse square distance from the primary body [5,6,7].

The assumption of constant mass is, in practice, somewhat restrictive and is well suited for propellantless spacecraft such as solar sail [7] or electric solar wind sail [8]. In most cases, however, the propulsive acceleration is a function of the current value of the spacecraft mass, which varies with time as the propellant is used. The analysis of this time-dependent situation has been tackled in the literature a few times, with the noteworthy exception of the special case in which the propulsion system is modulated in such a way to balance the mass variation of the spacecraft and obtain a propulsive acceleration either constant or proportional to the local gravity, see Boltz [5].

The main contribution of this paper is to fill this deficiency by means of new results in graphical or semi-analytical form. In fact, the availability of accurate approximations of exact solutions is important for the preliminary design of orbit transfers and for providing initial guesses for trajectory optimization purposes [9].

The radial acceleration problem is characterized by the existence of a simple and meaningful constant of motion, that is, the conservation of the angular momentum per unit mass, which also provides an important analogy with the Keplerian model. On the other hand, the presence of a time dependent mass in the equations of motion introduces a significant complication in the study of spacecraft trajectory. In fact, the resulting differential equation of motion is no longer autonomous and, as such, a first integral of motion for the radial velocity is difficult to be found [4].

This paper proposes a new methodology that guarantees a simple and quick solution for the radial acceleration problem for a spacecraft whose total mass decreases with time. In particular, two mission cases are discussed, according to whether the thrust modulus is constant or it varies with the inverse square distance from the primary. In the first case a graphical approach is discussed to find the spacecraft performance during an escape mission from the gravitational attraction of the primary. In the second case the polar equation of spacecraft trajectory is found, in an analytical form, using the trigonometric integral functions. These results are shown to be able to model the dynamics of a spacecraft with an electric or a Mini-Magnetospheric Plasma Propulsion system (M2P2) [10,11].

Consider a spacecraft, with mass m_0, which initially moves in a circular, Keplerian, parking orbit of radius r_0 around a primary body of gravitational parameter μ. Assume that the spacecraft primary propulsion system, when switched on, provides an outward, continuous, radial thrust. Since the thrust vector $\boldsymbol{T}$ is aligned, at each time, with the primary-spacecraft direction, the angular momentum $\boldsymbol{h}$ of the osculating orbit is a constant of motion and its modulus h, during the powered flight, can be simply expressed as

$$h = h_0 \triangleq \sqrt{\mu\, r_0} \tag{1}$$

where h_0 is the angular momentum along the initial orbit. Note that Eq. (1) holds independent of the way the thrust modulus varies with time.

As a consequence of the radial thrust assumption, the spacecraft motion can be suitably described within a two-dimensional reference frame whose fundamental plane coincides with the (fixed) plane of the osculating orbit. To this end, introduce a polar reference frame $\mathcal{T}(O; r, \theta)$ with origin in the center-of-mass O of the primary body. The spacecraft equations of motion are (see also Fig. 1):

$$\dot{r} = u \tag{2}$$

$$\dot{\theta} = \frac{\sqrt{\mu\, r_0}}{r^2} \tag{3}$$

$$\dot{u} = -\frac{\mu}{r^2} + \frac{\mu\, r_0}{r^3} + \frac{T}{m} \tag{4}$$

where u is the radial component of the spacecraft velocity, $T \triangleq \|\boldsymbol{T}\|$ is the propulsive thrust modulus, θ is the polar angle measured anticlockwise from

the primary body-spacecraft position at the beginning of the powered phase of flight, and m is the spacecraft instantaneous mass. From Eq. (1), the cir-

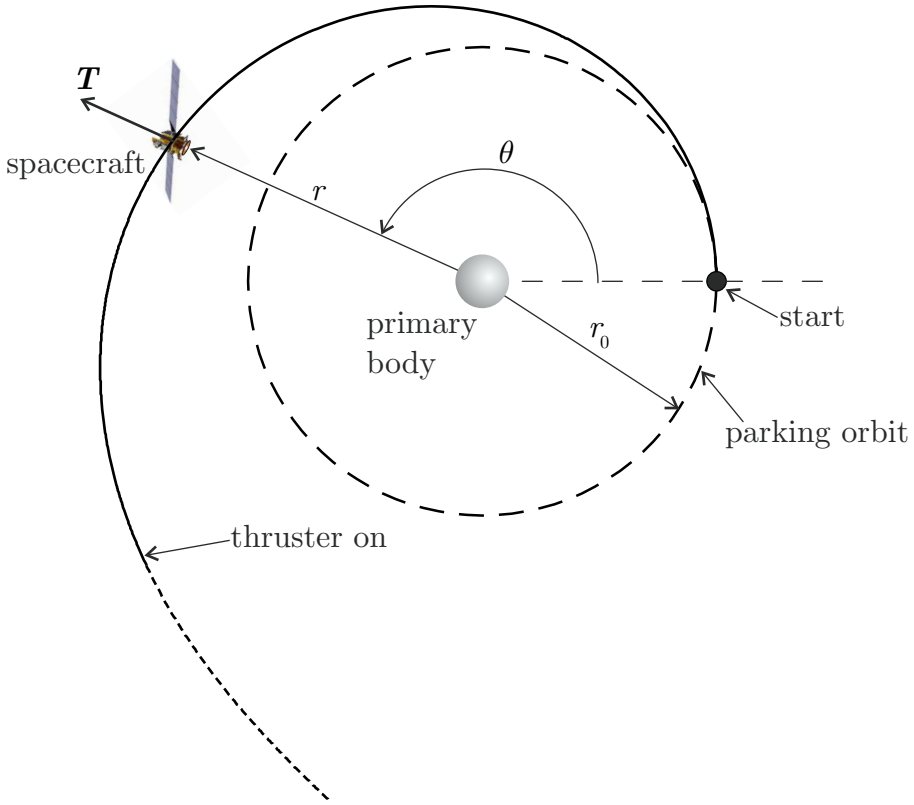

Figure 1. Reference frame and problem's parameters.

cumferential component of the spacecraft velocity is simply given by

$$v = \frac{h_0}{r} \equiv \frac{\sqrt{\mu\, r_0}}{r} \tag{5}$$

The last term in Eq. (4) represents the modulus of the propulsive acceleration $a \triangleq T/m$, whose value depends on the way the thrust and the spacecraft mass vary with time. Two special cases, of great practical interest, will be considered with the aim of modeling the behavior of a spacecraft equipped with an electric thruster. In particular, the electric power given to the propulsion system will be assumed to be either constant or varying with the inverse square distance r from the primary. Moreover, it will be shown that, under

mild additional assumptions, the proposed model can be used also for the analysis of an interplanetary mission for a spacecraft equipped with a M2P2.

2 Constant propulsive thrust and constant propellant mass flow rate

Assume first that the thrust modulus T remains constant and that the spacecraft mass decreases linearly with time. The mass variation is therefore described by

$$\dot{m} = -\frac{T}{v_e} \tag{6}$$

where v_e is a given constant parameter, with the dimensions of a velocity, whose value depends on the characteristics of the propulsion system. Note that Eq. (6) models the behavior of an electric propulsion system when the electric power does not vary with time. This happens, for example, for a nuclear electric power system. In this case v_e corresponds to the effective exhaust velocity, which is directly related to the thruster specific impulse [12]. The same relationship (6) can be applied to a solar electric propulsion system when the spacecraft moves around a celestial body whose distance from the Sun does not change significantly during the propelled mission phase.

Notably Eq. (6) can also be used to describe the working of an M2P2-based space vehicle that uses a nuclear power source [7,13]. According to Winglee [10,11], in an M2P2 thruster the propellant is transformed into plasma by means of a suitable source of electric power, thus creating an artificial magnetosphere around the spacecraft. Such a magnetosphere, by interacting with the solar wind, produces a propulsive thrust when the spacecraft operates in the deep space (that is, when it is far enough from possible planetary magnetospheres).

The resulting acceleration is essentially radially directed with respect to the Sun, even if experimental tests have shown the feasibility of generating an off-axis thrust of a few degrees [13], thus guaranteeing a (reduced) maneuver capability to the spacecraft.

Returning to Eq. (6), for an M2P2 thruster the term v_e represents a constant parameter, different from the effective exhaust velocity of an electric thruster. This parameter defines the propellant mass flow necessary to obtain a given propulsive thrust. For example, according to Refs. [10,13,14], an M2P2 thruster is potentially able to provide a thrust modulus $T = 1\,\mathrm{N}$ using a mass flow rate of about $|\dot{m}| = 0.5\,\mathrm{kg/day}$. This value corresponds to an equivalent effective exhaust velocity of $v_e = 172.8\,\mathrm{km/s}$.

For the following dynamical analysis, the equations of motions (2)–(4) and (6) can be conveniently transformed in a dimensionless form using the initial spacecraft mass m_0 as the reference unit of mass, the parking orbit radius r_0 as the unit of distance, and selecting the unit of time in such a way that the gravitational parameter μ is unitary. More precisely, introduce the dimensionless (with a tilde superscript) quantities:

$$\widetilde{r} \triangleq \frac{r}{r_0} \quad , \quad \widetilde{u} \triangleq \frac{u}{\sqrt{\mu/r_0}} \quad , \quad \widetilde{m} \triangleq \frac{m}{m_0} \quad , \quad \widetilde{a}_0 \triangleq \frac{a_0}{\mu/r_0^2} \quad , \quad \widetilde{v}_e \triangleq \frac{v_e}{\sqrt{\mu/r_0}} \tag{7}$$

where a_0 corresponds to the spacecraft propulsive acceleration when the thruster is switched on, that is, when the spacecraft distance from the primary is r_0 and its mass is m_0. In this case $a_0 = T/m_0$, where T is constant by assumption.

Using the dimensionless mass $\widetilde{m}$ in place of time t as the independent variable of the problem, the following nonlinear second order differential equation is

obtained combining Eqs. (2), (4) and (6)

$$\widetilde{r}'' = \frac{\widetilde{v}_e^2/\widetilde{a}_0^2}{\widetilde{r}^2}\left(\frac{1}{\widetilde{r}} - 1\right) + \frac{\widetilde{v}_e^2/\widetilde{a}_0}{\widetilde{m}} \tag{8}$$

where the prime symbol indicates a derivative with respect to $\widetilde{m}$. The previous differential equation is completed by two boundary conditions regarding the spacecraft position and velocity along the parking orbit, viz.

$$\widetilde{r}|_{\widetilde{m}=1} = 1 \quad , \quad \widetilde{r}'|_{\widetilde{m}=1} = 0 \tag{9}$$

In fact, the radial component of spacecraft velocity $u \triangleq \dot{r}$ can be written as

$$\frac{u}{r_0} = -\frac{T/m_0}{v_e}\,\widetilde{r}' \tag{10}$$

from which $\widetilde{r}' = 0$ on the parking orbit.

Even though no closed-form solution can be retrieved for Eq. (8), the use of $\widetilde{m}$ as the independent variable of the problem makes this equation particularly suitable for obtaining, via numerical simulations, the conditions under which an escape condition from the gravitational field of the primary may occur. Such a noteworthy mission scenario is the subject of the next section.

2.1 Escape conditions

An interesting question is to establish whether or not a spacecraft is able to escape from the gravitational field of the primary. To solve this problem, it is useful to first obtain an expression of the specific mechanical energy of the osculating orbit $\mathcal{E}$. From Eqs. (7) and (10), the dimensionless mechanical energy is

$$\widetilde{\mathcal{E}} \triangleq \frac{\mathcal{E}}{\mu/r_0} = \frac{1}{2}\left(\frac{\widetilde{a}_0\,\widetilde{r}'}{\widetilde{v}_e}\right)^2 + \frac{1}{2\,\widetilde{r}^2} - \frac{1}{\widetilde{r}} \tag{11}$$

Note that $\widetilde{\mathcal{E}} = -1/2$ along the initial orbit. For a given pair $\widetilde{a}_0$ and $\widetilde{v}_e$, that is, for a suitable combination of propulsion system characteristics and spacecraft mass (the latter being implicitly defined through $\widetilde{a}_0$), the equation of motion (8) can be numerically backward integrated within the interval $\widetilde{m} \in [1,\, 0)$, using the boundary conditions (9), until the escape condition $\widetilde{\mathcal{E}} = 0$ is met. The corresponding dimensionless escape distance $\widetilde{r}_{\rm esc}$ and spacecraft mass $\widetilde{m}_{\rm esc}$ can also be calculated. Clearly, the functions $\widetilde{r}_{\rm esc} = \widetilde{r}_{\rm esc}(\widetilde{a}_0, \widetilde{v}_e)$ and $\widetilde{m}_{\rm esc} = \widetilde{m}_{\rm esc}(\widetilde{a}_0, \widetilde{v}_e)$ describe three-dimensional surfaces that can be conveniently displayed through contour lines.

Before discussing the simulation results, a brief remark is useful. In the classical case of constant radial acceleration, that is, when T/m is constant for the whole mission length, an escape condition may occur only if $T/m > \mu/(8\, r_0^2)$, see Ref. [1]. Under such an assumption, it is known [3] that the escape distance satisfies the inequality $r_{\rm esc} < 5\, r_0$. If, in addition, the spacecraft trajectory may tolerate the presence of coasting phases, that is, the thruster may be freely switched off or on during the flight, the required thrust to attain an escape condition can be further decreased at the expense of an increase in mission time. The trade-off between thrust level and mission length is analyzed in Ref. [15].

The situation discussed in this section is substantially different from the classical case of constant thrust modulus. In fact, the propellant mass consumption described by Eq. (6) implies a continuous increase of the local propulsive acceleration $a = a_0/\widetilde{m}$. Therefore, an escape condition is possible, at least in mathematical terms, for any value of propulsive thrust modulus. In practice, however, the escape condition could correspond to an unacceptably small value

of $\widetilde{m}$. For this reason it is important to numerically analyze the influence of the pair $(\widetilde{a}_0, \widetilde{v}_e)$ on mission performance during an escape trajectory, which can be quantified in terms of values of $\widetilde{m}_{\rm esc}$ and $\widetilde{r}_{\rm esc}$ calculated at escape conditions.

A parametric study has been performed by varying the initial propulsive acceleration and the effective exhaust velocity in the range $\widetilde{a}_0 \in [0.01, 1]$ and $\widetilde{v}_e \in [1, 10]$, and integrating Eq. (8) with a variable order Adams-Bashforth-Moulton solver scheme [16] with absolute and relative errors of 10^{-12}. The resulting contour curves are illustrated in Figs. 2 and 3. In particular Fig. 2 shows the dimensionless spacecraft mass $\widetilde{m}_{\rm esc}$ and Fig. 3 represents the dimensionless distance $\widetilde{r}_{\rm esc}$ when the mechanical energy $\widetilde{\mathcal{E}}$ is zero. Recalling from Eq. (6) that the spacecraft mass decreases linearly with time, the information taken from Fig. 2 are sufficient to estimate, for a given pair $(\widetilde{a}_0, \widetilde{v}_e)$, the time $t_{\rm esc}$ required to reach an escape condition. In fact, from Eqs. (7), one obtains

$$t_{\rm esc} = \sqrt{\frac{r_0^3}{\mu}} \, \frac{\widetilde{v}_e}{\widetilde{a}_0} \, (1 - \widetilde{m}_{\rm esc}) \tag{12}$$

where $\widetilde{m}_{\rm esc}$ can be estimated in graphical form using Fig. 2. To summarize, Figs. 2 and 3 provide an overall view to the escape problem of a spacecraft with radial thrust of constant modulus. As such these figures represent an extension of the classical results by Tsien [1], in which the spacecraft total mass was assumed to remain constant during the flight.

A few comments are necessary about the "wave-like" behaviour in both the central and the lower part of Fig. 2 for the contour lines of $\widetilde{m}_{\rm esc} = \widetilde{m}_{\rm esc}(\widetilde{a}_0, \widetilde{v}_e)$. This phenomenon is especially marked for small values of the initial propulsive acceleration $\widetilde{a}_0$. In particular, a "wave-like" line appears when $\widetilde{a}_0 < 0.12$. The reason may be explained as follows. From an analysis of the numerical simulations, it turns out that in correspondence of pairs $(\widetilde{a}_0, \widetilde{v}_e)$ that define a point

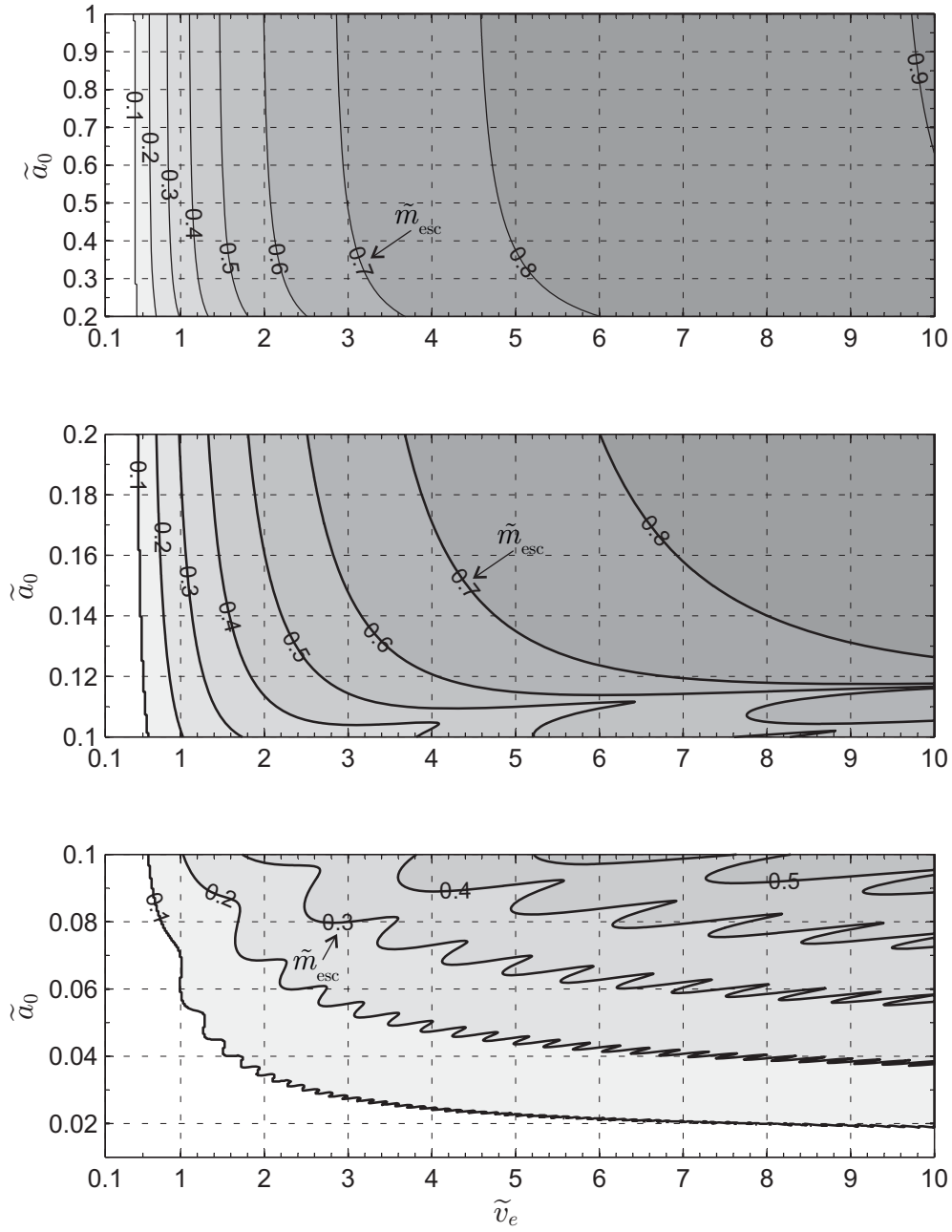

Figure 2. Escape dimensionless mass $\widetilde{m}_{\text{esc}}$ for a constant value of both propulsive thrust modulus and propellant mass flow rate.

close to one of these "waves", the escape trajectory is characterized by legs in which $u < 0$. In other terms, these trajectories are constituted by a sequence of three or more arcs in which a phase of departure from the primary body (when $u > 0$) is followed by an approach phase ($u < 0$). Clearly the number

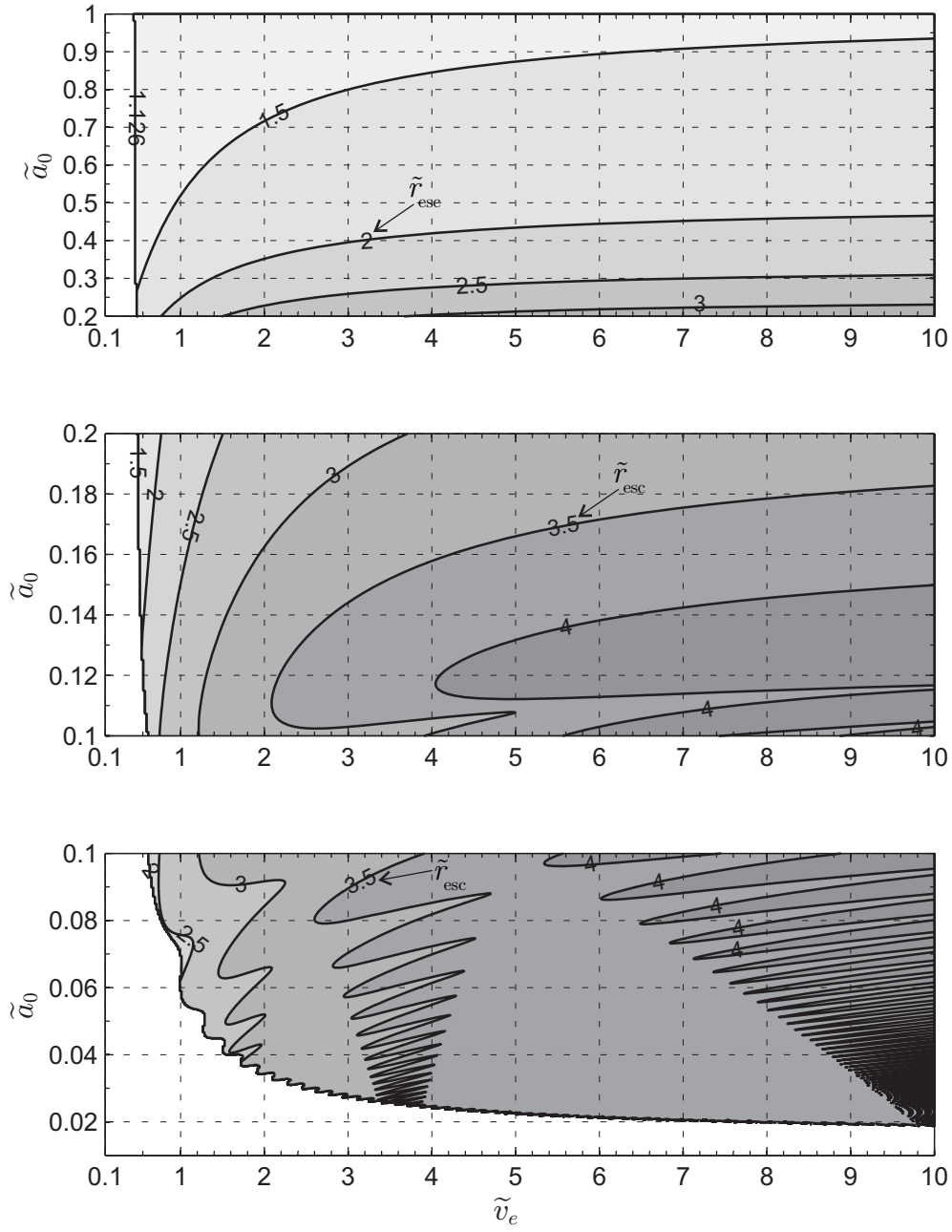

Figure 3. Escape dimensionless radius $\widetilde{r}_{\mathrm{esc}}$ for a constant value of both propulsive thrust modulus and propellant mass flow rate.

of arcs is always odd, and both the first and the last one correspond to a departure phase. This sequence of departure and approach arcs is highlighted in Fig. 4, which shows the time variation of the dimensionless distance when $\widetilde{a}_0 = 0.1$ and $\widetilde{v}_e = 6$, while the corresponding escape trajectory is illustrated

in Fig. 5.

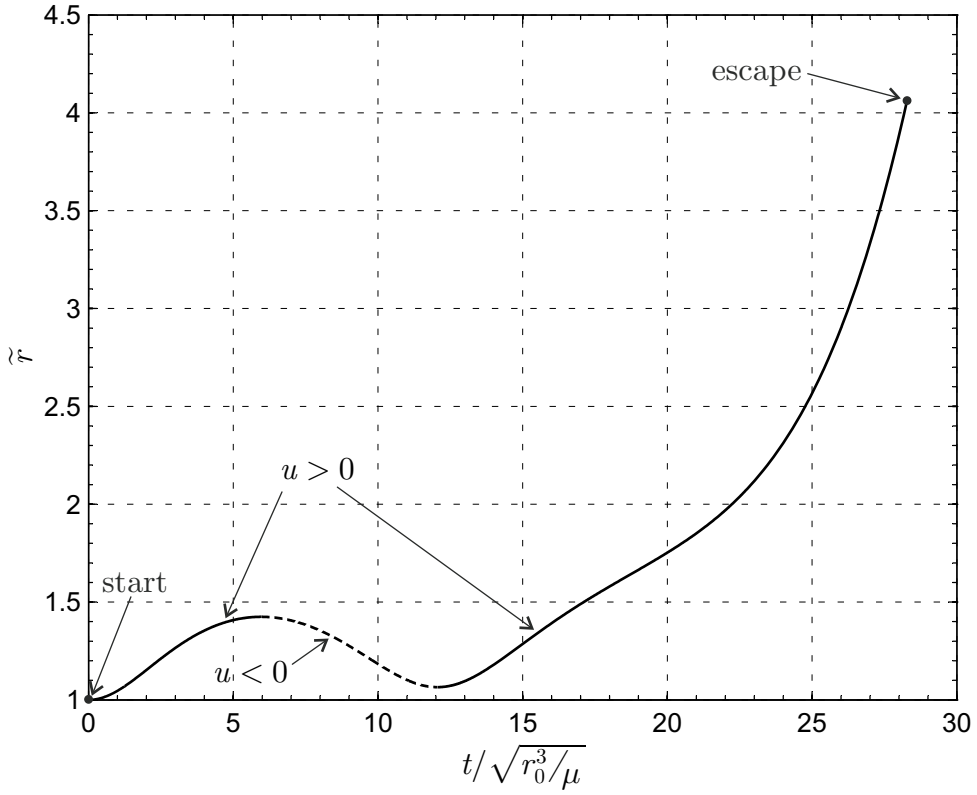

Figure 4. Time variation of the dimensionless radius when $\widetilde{a}_0 = 0.1$ and $\widetilde{v}_e = 6$.

This behavior is consistent with the results obtained from Prussing and Coverstone [2] and can be explained in terms of mechanical energy. In fact, for small values of $\widetilde{a}_0$ the spacecraft is initially trapped into the so called potential well [2]. If the propulsion acceleration remains constant, as in the classical case, an escape from the potential well cannot take place, and the spacecraft is constrained to orbit around the primary and to track a trajectory whose shape has been analytically studied in Ref. [4]. In the case of propellant mass that decreases linearly with time, as is assumed in this paper, the propulsive acceleration tends to increase monotonically and the spacecraft can therefore eventually escape from the potential well and meet the escape conditions. This is confirmed by Figs. 4 and 5, which show how an escape occurs for a spacecraft

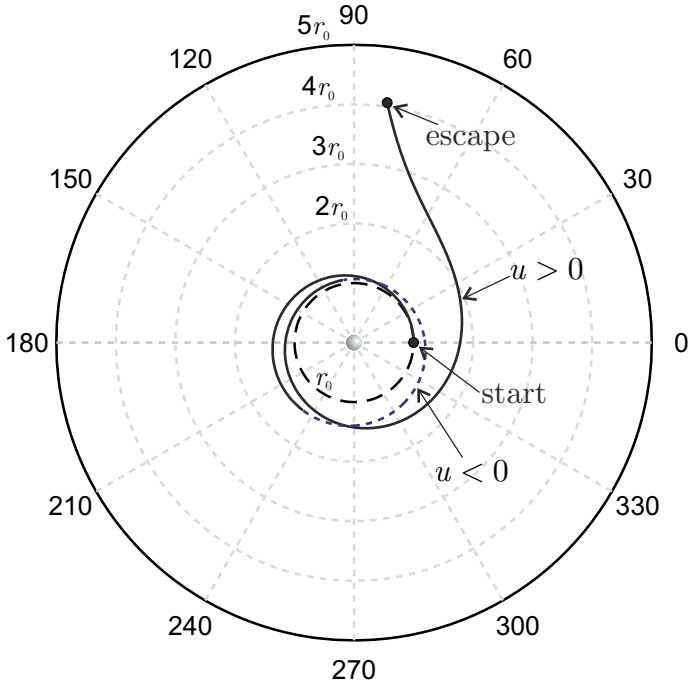

Figure 5. Escape trajectory when $\widetilde{a}_0 = 0.1$ and $\widetilde{v}_e = 6$.

whose initial dimensionless acceleration is less than 1/8.

2.2 Case Study

A numerical example is now discussed to highlight the effectiveness of the proposed mathematical model. Consider a spacecraft with an electric propulsion system having a specific impulse $I_{sp} = 3000\,\mathrm{s}$. The spacecraft is initially placed in a geostationary orbit, characterized by $\mu = \mu_\oplus \triangleq 3.986 \times 10^5\,\mathrm{km}^3/\mathrm{s}^2$ and $r_0 \simeq 42164\,\mathrm{km}$. In this case $v_e = g\,I_{sp} \simeq 29420\,\mathrm{m/s}$, where $g \triangleq 9.806\,\mathrm{m/s}^2$ is the standard gravity, and from the last of Eqs. (7), $\widetilde{v}_e \simeq 9.57$. Assume that the escape condition is obtained with a propellant mass fraction of 30%, that is, with a dimensionless mass $\widetilde{m}_{\mathrm{esc}} = 0.7$. From Fig. 2 the required value of initial acceleration would be $\widetilde{a}_0 \simeq 0.12$, which corresponds to an initial acceleration modulus $T/m_0 \simeq 26.9\,\mathrm{mm/s}^2$, see the third of Eqs. (7). For an

initial spacecraft mass $m_0 = 500\,\mathrm{kg}$ the required propulsive thrust would be $T \simeq 13.5\,\mathrm{N}$, an enormous value, well beyond the technical capabilities of an electric thruster [12]. Even though such a large thrust requirement could be partially reduced by increasing the propellant mass fraction, Fig. 2 confirms that a radial thrust strategy is rather inefficient to attain an escape condition as long as the thruster is switched on during the whole mission (that is, no coasting phases are allowed). Of course a different thrust strategy, such as a circumferential thrust, could be more efficient in terms of propellant consumption, even if it would require a higher thrust steering capability.

The situation is much different if a Solar System escape mission is performed using an M2P2-based spacecraft. Note that in this case the radial thrust strategy is justified by the reduced steering capability of this kind of thruster. Also, the radial model well approximates the real spacecraft behavior [13]. According to the previous discussion, a reasonable value of the equivalent effective exhaust velocity for an M2P2 thruster is $v_e = 172.8\,\mathrm{km/s}$. Assume, for example, an initial heliocentric parking orbit with radius $r_0 = 1\,\mathrm{au}$, which amounts to escaping from Earth with zero hyperbolic excess velocity with respect to the planet. In this case $\widetilde{v}_e \simeq 5.8$, since $\mu = \mu_\odot \triangleq 132712439935.5\,\mathrm{km}^3/\mathrm{s}^2$. Assuming, again, that the escape condition is met with a propellant mass fraction of 30%, from Fig. 2 the required dimensionless acceleration is about $\widetilde{a}_0 = 0.125$. Because $\mu/r_0^2 \simeq 5.93\,\mathrm{mm/s}^2$ along the parking orbit, the initial propulsive acceleration is $a_0 \simeq 0.74\,\mathrm{mm/s}^2$. For an initial spacecraft mass of $m_0 = 1000\,\mathrm{kg}$, the required propulsive thrust is $T \simeq 0.74\,\mathrm{N}$, a value that, according to Winglee, is regarded to be technically feasible [10,11,14]. From Fig. 3 the escape conditions are met for a dimensionless distance slightly greater than 4, which means $r_{\mathrm{esc}} = \widetilde{r}_{\mathrm{esc}}\, r_0 \simeq 4.2\,\mathrm{au}$, a value smaller than the mean Sun-

Jupiter distance. This is confirmed by Fig. 6, which shows the results obtained from the numerical integration of equations of motion (2)–(4) and (6). The heliocentric trajectory tracked by the spacecraft is illustrated in Fig. 7. Note that the escape condition indeed takes place at a distance $4.2\,r_0$ after about 14 time units (in fact, from Eq. (12) $\widetilde{t}_{\rm esc} \simeq 13.92$).

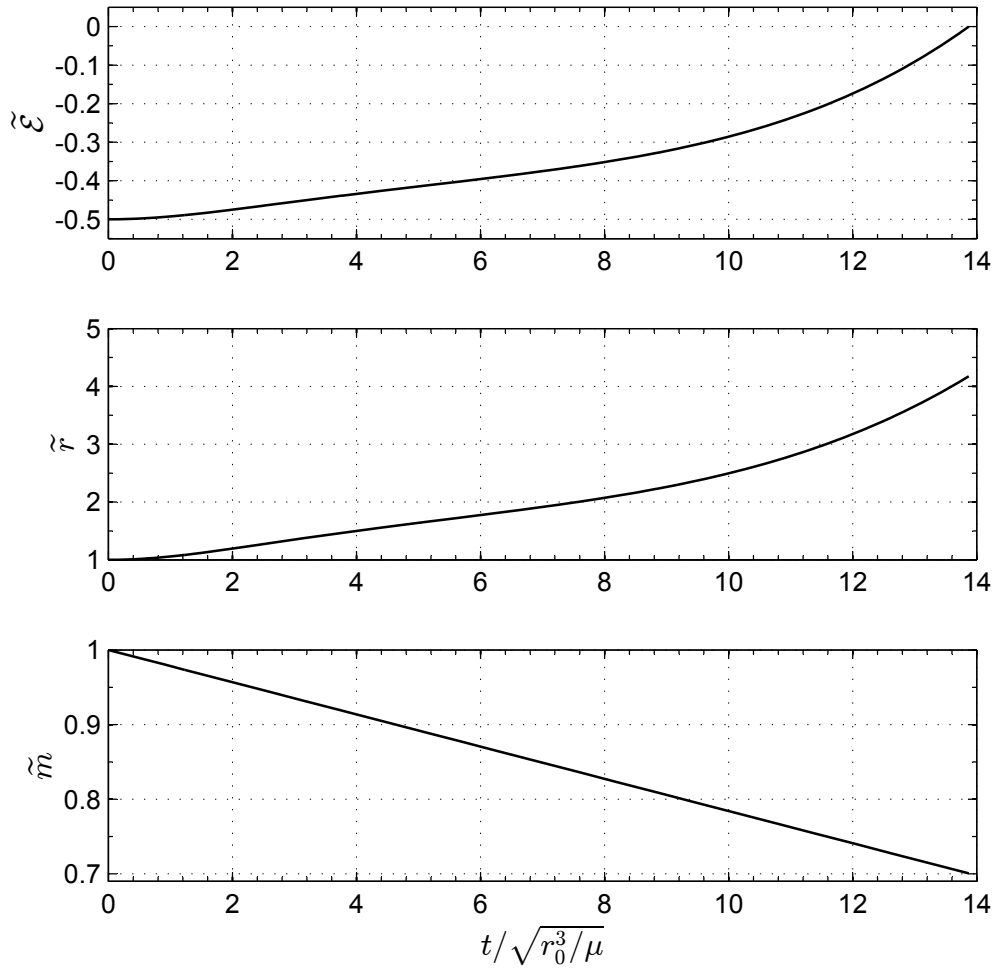

Figure 6. Numerical simulations for a Solar System escape mission using an M2P2-based spacecraft with $\widetilde{m}_{\rm esc} = 0.7$ (constant thrust modulus).

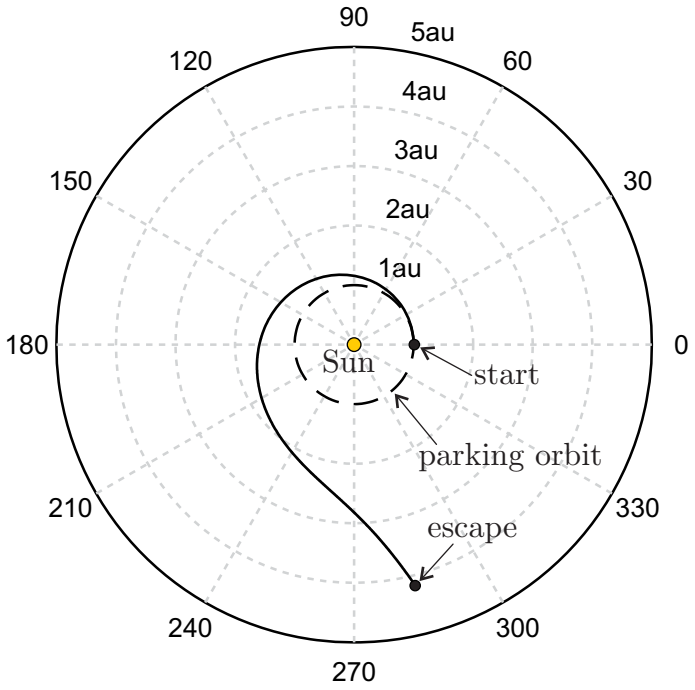

Figure 7. Solar System escape trajectory of an M2P2-based spacecraft with $\widetilde{m}_{\rm esc} = 0.7$ (constant thrust modulus).

3 Thrust and mass flow rate that change with distance

In this second mission scenario the thrust modulus T and the propellant mass flow rate $\dot{m}$ are both proportional to the inverse square distance from the primary. This situation is representative of an interplanetary mission for a spacecraft equipped with a solar electric propulsion system [17,18], or with an M2P2 thruster whose power generation system is based on photovoltaic panels. In fact, within a first order approximation model, the electric power from the photovoltaic panels in the interplanetary space scales as $1/r^2$, where r is the distance from the Sun [19,20,21].

From a mathematical viewpoint, in this case the propulsive acceleration and

the spacecraft mass variation are described as

$$\frac{T}{m} = \frac{a_0}{\widetilde{m}\,\widetilde{r}^2} \qquad , \qquad \dot{m} = -\frac{m_0\, a_0}{v_e\, \widetilde{r}^2} \tag{13}$$

where $\widetilde{m}$ and $\widetilde{r}$ are defined in Eq. (7).

Introduce now the dimensionless length $\rho \triangleq r_0/r \equiv 1/\widetilde{r}$, which is equal to the reciprocal of $\widetilde{r}$. From the second of Eqs. (13), the following relationships are found:

$$u = \frac{r_0\, a_0}{v_e}\, \rho' \qquad , \qquad \dot{u} = -\frac{r_0\, a_0^2}{v_e^2}\, \rho''\, \rho^2 \tag{14}$$

where the prime symbol denotes, again, a derivative taken with respect to the dimensionless mass $\widetilde{m}$. Substituting the second of (13) and the second of (14) into the equation of motion (4), one obtains:

$$\frac{r_0\, a_0^2}{v_e^2}\, \rho'' = \frac{\mu}{r_0^2}\, (1 - \rho) - \frac{a_0}{\widetilde{m}} \tag{15}$$

Taking into account the relationships (7), an equivalent, compact, form of the last equation is

$$\left(\frac{\widetilde{a}_0}{\widetilde{v}_e}\right)^2 \rho'' = 1 - \rho - \frac{\widetilde{a}_0}{\widetilde{m}} \tag{16}$$

This second order nonlinear differential equation is completed by a set of two boundary conditions, which model the spacecraft position and velocity in the initial parking orbit of radius r_0, viz.

$$\rho|_{\widetilde{m}=1} = 1 \quad , \quad \rho'|_{\widetilde{m}=1} = 0 \tag{17}$$

Note that the second condition, corresponding to a radial velocity equal to zero (that is, $u = 0$), is a consequence of the first of Eqs. (14).

The previous differential equation (16) along with its boundary conditions (17) can be solved using the sine integral function $\mathrm{Si}(z)$ and the cosine integral function $\mathrm{Ci}(z)$, defined as

$$\mathrm{Si}(z) \triangleq \int_0^z \frac{\sin y}{y}\,\mathrm{d}y \tag{18}$$

$$\mathrm{Ci}(z) \triangleq \gamma + \ln(z) + \int_0^z \frac{\cos y - 1}{y}\,\mathrm{d}y \tag{19}$$

where γ is Euler's constant. Note that a number of computer routines are available to calculate these integrals in a fast and accurate way, see Ref. [22]. The solution of Eq. (16) can be written as

$$\rho = \widetilde{v}_e \left\{ \sin\left(\frac{\widetilde{m}\,\widetilde{v}_e}{\widetilde{a}_0}\right) \left[\mathrm{Ci}\left(\frac{\widetilde{v}_e}{\widetilde{a}_0}\right) - \mathrm{Ci}\left(\frac{\widetilde{m}\,\widetilde{v}_e}{\widetilde{a}_0}\right)\right] + \cos\left(\frac{\widetilde{m}\,\widetilde{v}_e}{\widetilde{a}_0}\right) \left[\mathrm{Si}\left(\frac{\widetilde{m}\,\widetilde{v}_e}{\widetilde{a}_0}\right) - \mathrm{Si}\left(\frac{\widetilde{v}_e}{\widetilde{a}_0}\right)\right]\right\} + 1 \tag{20}$$

while the derivative ρ', necessary for calculating the radial velocity u, is given by

$$\rho' = \frac{\widetilde{v}_e^2}{\widetilde{a}_0} \left\{ \cos\left(\frac{\widetilde{m}\,\widetilde{v}_e}{\widetilde{a}_0}\right) \left[\mathrm{Ci}\left(\frac{\widetilde{v}_e}{\widetilde{a}_0}\right) - \mathrm{Ci}\left(\frac{\widetilde{m}\,\widetilde{v}_e}{\widetilde{a}_0}\right)\right] + \sin\left(\frac{\widetilde{m}\,\widetilde{v}_e}{\widetilde{a}_0}\right) \left[\mathrm{Si}\left(\frac{\widetilde{v}_e}{\widetilde{a}_0}\right) - \mathrm{Si}\left(\frac{\widetilde{m}\,\widetilde{v}_e}{\widetilde{a}_0}\right)\right]\right\} \tag{21}$$

Equations (20)-(21) give a closed-form, parametric description (as a function of $\widetilde{m}$) of the spacecraft dynamics during the propelled flight phase.

To represent the spacecraft trajectory in a polar reference frame $\mathcal{T}(O; r, \theta)$, it is necessary to find an expression of the distance r and the anomaly θ for a given value of the dimensionless mass $\widetilde{m} \in [1,\, 0)$. To this end, observe that

the distance can be written as

$$r(\widetilde{m}) = \frac{r_0}{\widetilde{v}_e \left\{ \sin\left(\frac{\widetilde{m}\,\widetilde{v}_e}{\widetilde{a}_0}\right) \left[\mathrm{Ci}\left(\frac{\widetilde{v}_e}{\widetilde{a}_0}\right) - \mathrm{Ci}\left(\frac{\widetilde{m}\,\widetilde{v}_e}{\widetilde{a}_0}\right) \right] + \cos\left(\frac{\widetilde{m}\,\widetilde{v}_e}{\widetilde{a}_0}\right) \left[\mathrm{Si}\left(\frac{\widetilde{m}\,\widetilde{v}_e}{\widetilde{a}_0}\right) - \mathrm{Si}\left(\frac{\widetilde{v}_e}{\widetilde{a}_0}\right) \right] \right\} + 1} \tag{22}$$

Consider now the anomaly θ. Combining Eq. (3) and the second of Eqs. (13) one obtains

$$\theta' = -\frac{\widetilde{v}_e}{\widetilde{a}_0} \tag{23}$$

which can be simply integrated to get

$$\theta(\widetilde{m}) = \frac{\widetilde{v}_e}{\widetilde{a}_0} \left(1 - \widetilde{m}\right) \tag{24}$$

In fact, recall that $\widetilde{a}_0$ and $\widetilde{v}_e$ are constant and, by assumption, θ is zero at the beginning of the propelled phase. Equation (24) states that the anomaly varies linearly with the spacecraft mass.

The polar equation of the trajectory can now be recovered by writing $\widetilde{m}$ as a function of θ from Eq. (24) and then substituting the obtained expression of $\widetilde{m}$ into Eq. (22). The result is:

$$r = \frac{r_0}{\widetilde{v}_e \left\{ \sin\left(\frac{\widetilde{v}_e}{\widetilde{a}_0} - \theta\right) \left[\mathrm{Ci}\left(\frac{\widetilde{v}_e}{\widetilde{a}_0}\right) - \mathrm{Ci}\left(\frac{\widetilde{v}_e}{\widetilde{a}_0} - \theta\right) \right] + \cos\left(\frac{\widetilde{v}_e}{\widetilde{a}_0} - \theta\right) \left[\mathrm{Si}\left(\frac{\widetilde{v}_e}{\widetilde{a}_0} - \theta\right) - \mathrm{Si}\left(\frac{\widetilde{v}_e}{\widetilde{a}_0}\right) \right] \right\} + 1} \tag{25}$$

In particular, at the beginning of the transfer (that is, when $\theta = 0$), the previous equation returns the correct value $r = r_0$.

3.2 Escape conditions

To calculate the escape conditions from the primary, it is first useful to find an expression for u and v for a given value of $\widetilde{m}$ (equivalently, from Eq. (24), for a given anomaly θ). Combining Eqs. (5) and (14) with (20) and (21) it can

be verified that

$$u = \sqrt{\frac{\mu}{r_0}}\,\frac{\widetilde{a}_0}{\widetilde{v}_e}\,\rho' \qquad , \qquad v = \sqrt{\frac{\mu}{r_0}}\,\rho \tag{26}$$

from which the mechanical energy can be written as

$$\widetilde{\mathcal{E}} = \frac{1}{2}\left(\frac{\widetilde{a}_0\,\rho'}{\widetilde{v}_e}\right)^2 + \frac{\rho^2}{2} - \rho \tag{27}$$

As usual, an escape condition occurs when $\widetilde{\mathcal{E}} = 0$. According to Boltz [5] and McInnes [7] recall that for a spacecraft of constant mass, whose radial thrust varies as the inverse square distance from the primary, an escape condition is possible only if $a_0 \geq 0.5\,\mu/r_0^2$. The escape condition can also be met for smaller values of the initial propulsive acceleration at the expense of a more complex thrust strategy, that is, including coasting phases [6,23].

Unlike the case of constant mass, the results obtained when $\dot{m}$ depends on r are substantially different. First note from Eq. (27) that the escape problem is now simply reduced to that of finding the root of a nonlinear function. The numerical results have been summarized in Fig. 8. In particular, Fig. 8 shows that when the spacecraft mass decreases with time, an escape condition can, in principle, always be met. This result is similar to what has been obtained for the previous case of constant propulsive thrust and constant propellant mass flow rate.

4 Conclusions

A new method has been discussed for the study of the motion of a spacecraft subjected to a continuous radial thrust. Unlike the classical problem in which the spacecraft mass is assumed to remain constant, the proposed approach takes into account the effect of a mass decrease due to propellant consumption.

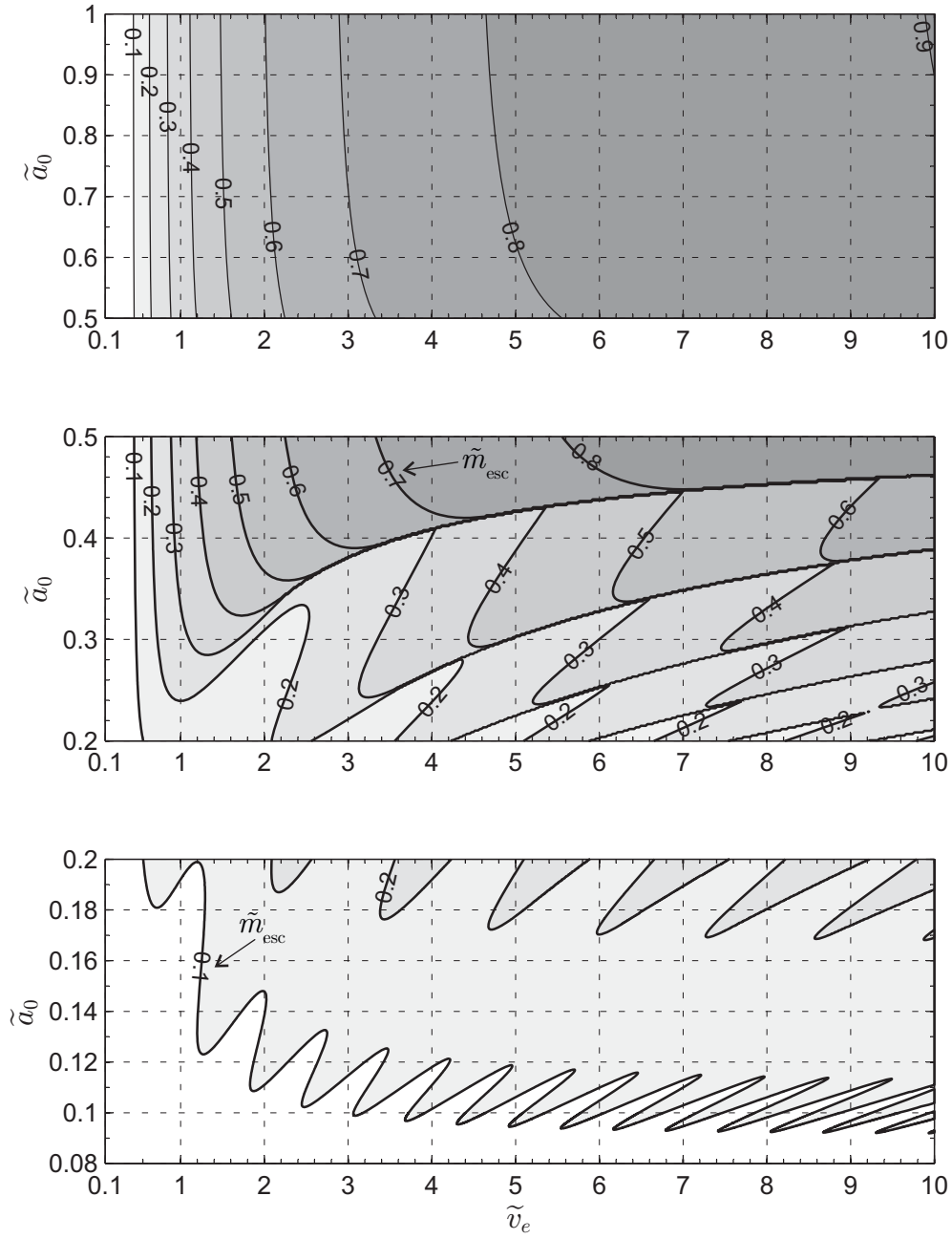

Figure 8. Escape dimensionless mass $\widetilde{m}_{\text{esc}}$ for a thrust modulus that varies proportional to $1/r^2$.

Using a suitable mathematical transformation, the spacecraft dynamics can be fully described by means of a single nonlinear second order differential equation in which the primary-spacecraft distance is expressed as a function of the vehicle's actual mass.

Two different mission scenarios have been discussed, one where both the propulsive thrust modulus and the propellant mass flow rate are constant along the whole mission, the other with the thrust modulus and the mass flow rate that vary inversely proportional to the distance between the spacecraft and the primary body. In the first case a graphical solution is discussed for evaluating the performance during an escape mission. For a given propellant mass fraction at the end of mission and a given value of effective exhaust velocity, the thrust modulus required to fulfill the mission can be easily calculated in graphical form, along with the corresponding escape distance and the total flight time. In the second case a closed-form solution, which uses the trigonometric integral functions, has been found for the description of the spacecraft dynamics during the propelled flight phase. The two mission scenarios are representative of either an electric thruster or a mini-magnetospheric propulsion system, and some examples have been discussed to confirm the effectiveness of the methodology for a preliminary mission analysis.

A natural extension of this work should include the case in which the spacecraft mass has a discontinuity during the escape trajectory. This case is representative of a mission scenario in which a part of the spacecraft (for example, a stage of the propulsion system or a propellant tank) is jettisoned during the transfer trajectory.

References

[1] H. S. Tsien, Take-off from satellite orbit, Journal of the American Rocket Society 23 (4) (1953) 233–236, doi: 10.2514/8.4599.

[2] J. E. Prussing, V. L. Coverstone, Constant radial thrust acceleration redux,

Journal of Guidance, Control, and Dynamics 21 (3) (1998) 516–518, doi: 10.2514/2.7609.

[3] R. H. Battin, An Introduction to the Mathematics and Methods of Astrodynamics, AIAA, New York, 1987, pp. 408–415, ISBN: 1-563-47342-9.

[4] A. A. Quarta, G. Mengali, New look to the constant radial acceleration problem, Journal of Guidance, Control, and Dynamics 35 (3) (2012) 919–929, doi: 10.2514/1.54837.

[5] F. W. Boltz, Orbital motion under continuous radial thrust, Journal of Guidance, Control, and Dynamics 14 (3) (1991) 667–670, doi: 10.2514/3.20690.

[6] H. Yamakawa, Optimal radially accelerated interplanetary trajectories, Journal of Spacecraft and Rockets 43 (1) (2006) 116–120, doi: 10.2514/1.13317.

[7] C. R. McInnes, Orbits in a generalized two-body problem, Journal of Guidance, Control, and Dynamics 26 (5) (2003) 743–749, doi: 10.2514/2.5129.

[8] G. Mengali, A. A. Quarta, G. Aliasi, A graphical approach to electric sail mission design with radial thrust, Acta Astronautica 82 (2) (2013) 197–208, doi: 10.1016/j.actaastro.2012.03.022.

[9] A. E. Petropoulos, J. A. Sims, A review of some exact solutions to the planar equations of motion of a thrusting spacecraft, in: 2nd International Symposium on Low-Thrust Trajectory (LoTus-2), Toulouse, France, 2002, available online (cited July 7, 2013) `http://hdl.handle.net/2014/8673`.

[10] R. M. Winglee, P. Euripides, T. Ziemba, J. Slough, L. Giersch, Simulation of mini-magnetospheric plasma propulsion (M2P2) interacting with an external plasma wind, in: 39th Joint Propulsion Conference and Exhibition, AIAA Paper 2003-5225, Huntsville, 2003.

[11] R. M. Winglee, J. Slough, T. Ziemba, A. Goodson, Mini-magnetospheric plasma

propulsion: Tapping the energy of the solar wind for spacecraft propulsion, Journal of Geophysical Research 105 (A9) (2000) 21,067–21,078 .

[12] G. P. Sutton, O. Biblarz, Rocket Propulsion Elements, 7th Edition, Wiley-Interscience, 2000, Ch. 19, ISBN: 0-471-32642-9.

[13] A. J. Trask, W. J. Mason, V. L. Coverstone, Optimal interplanetary trajectories using constant radial thrust and gravitational assists, Journal of Guidance, Control, and Dynamics 27 (3) (2004) 503–506, doi: 10.2514/1.2586.

[14] R. Winglee, J. Slough, T. Ziemba, A. Goodson, Mini-magnetospheric plasma propulsion (M2P2): High speed propulsion sailing the solar wind, in: Space Technology and Applications International Forum - 2000, Albuquerque, New Mexico (USA), 2000, pp. 962–967, AIP Conf. Proc. 504.

[15] A. A. Quarta, G. Mengali, Optimal switching strategy for radially accelerated trajectories, Celestial Mechanics and Dynamical Astronomy 105 (4) (2009) 361–377, doi: 10.1007/s10569-009-9233-2.

[16] L. F. Shampine, M. W. Reichelt, The MATLAB ODE suite, SIAM Journal on Scientific Computing 18 (1) (1997) 1–22, doi: 10.1137/S1064827594276424.

[17] G. Mengali, A. A. Quarta, Fuel-optimal, power-limited rendezvous with variable thruster efficiency, Journal of Guidance, Control, and Dynamics 28 (6) (2005) 1194–1199, doi: 10.2514/1.12480.

[18] M. D. Rayman, S. N. Williams, Design of the first interplanetary solar electric propulsion mission, Journal of Spacecraft and Rockets 39 (4) (2002) 589–595, doi: 10.2514/2.3848.

[19] C. G. Sauer, Jr, K. G. Atkins, Potential advantages of solar electric propulsion for outer planet orbiters, in: AIAA 9th Electric Propulsion Conference, Bethesda, MD, 1972, AIAA Paper 72-423.

[20] C. G. Sauer, Jr., Solar electric performance for medlite and delta class planetary missions, in: AAS/AIAA Astrodynamics Specialist Conference, 1997, aAS Paper 97-726.

[21] C. G. Sauer, Jr., Modeling of thruster and solar array characteristics in the jpl low-thrust trajectory analysis, in: 13th International Electric Propulsion Conference, San Diego, CA, 1978, AIAA Paper 78-645.

[22] W. H. Press, S. A. Teukolsky, W. T. Vetterling, B. P. Flannery, Numerical Recipes: The Art of Scientific Computing, Cambridge University Press, New York, 2007, pp. 300–302.

[23] A. A. Quarta, G. Mengali, Analytical results for solar sail optimal missions with modulated radial thrust, Celestial Mechanics and Dynamical Astronomy 109 (2) (2011) 147–166, doi: 10.1007/s10569-010-9319-x.